EurJIC
European Journal of Inorganic Chemistry

Research Article
doi.org/10.1002/ejic.202200509

Chemistry Europe
European Chemical Societies Publishing

www.eurjic.org

Dinuclear Copper(I) Complexes Supported by Bis-Tridentate *N*-Donor-Ligands: Turning-On Tyrosinase Activity

Rebecca Schneider,[a] Tobias A. Engesser,[a] Jessica N. Hamann,[a] Christian Näther,[a] and Felix Tuczek*[a]

Four structurally related bis-tridentate *N*-donor ligands with either two secondary amine or two imine functions were synthesized, and the corresponding dicopper(I) complexes were investigated as catalysts for the tyrosinase-like conversion of 2,4-di-*tert*-butylphenol (DTBP-H) to 3,5-di-*tert*-butylquinone (DTBQ). Notably, the imine systems show evidence for both a μ-η^2:η^2-peroxo-dicopper(II) species and catalytic conversion of DTBP-H to DTBQ. Moreover, kinetic studies indicate that a dinuclear copper-oxygen species is involved in the monooxygenation of DTBP-H. In contrast, the amine systems do not show monooxygenase activity. Comparison of the experimentally determined catalytic activities with DFT-optimized geometries of μ-η^2:η^2-peroxo-dicopper(II) intermediates suggests that the ligand rigidity of the imine systems allows equatorial attack of the substrate and, thus, subsequent monooxygenation whereas this is not possible in the amine systems due to the fact that no free equatorial positions are available in the μ-peroxo intermediate.

Introduction

The pigment melanin is involved in numerous biological protective processes in nature like the coloring of skin, wound healing, immune response and browning of fruit and vegetables.[1] The first step of its biosynthesis is mediated by the type 3 copper protein tyrosinase (TY). This ubiquitous enzyme catalyzes the monooxygenation of L-tyrosine to L-DOPAquinone (Scheme 1 a).[2–6] In contrast, the related enzyme catechol oxidase (CO) is only capable of the two-electron oxidation of *o*-diphenols to the corresponding *o*-quinones (Scheme 1 a).[5–8] The dinuclear copper centre of both enzymes binds dioxygen in a characteristic fashion, forming a μ-η^2:η^2-peroxo-dicopper(II) species that reacts with the phenolic substrates.[2,4,6,7] Over the years, more and more insights into the underlying mechanisms have been gained with the help of biochemical studies on the enzymes, protein X-ray crystallography and the investigation of synthetic models.[2,6,7,9] Influences of the ligand design, the counter ions and the used substrates on the reactivity of small-molecule model systems have been investigated in depth, making use of a growing library of

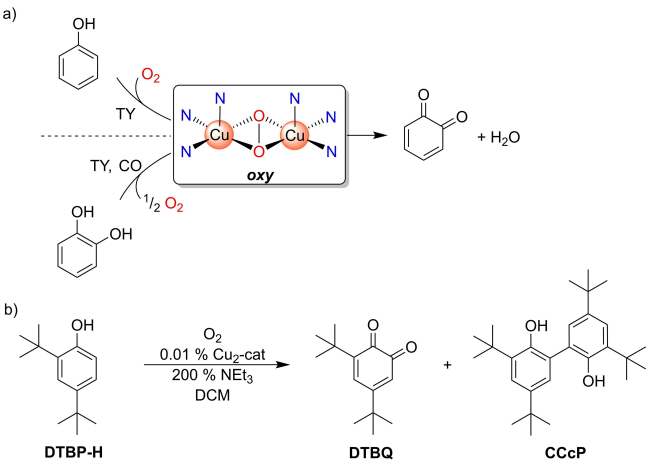

Scheme 1. a) Conversion of monophenols resp. catechols to *o*-quinones mediated by the *oxy*-form (centre) of the enzymes tyrosinase (TY) resp. catechol oxidase (CO); b) Catalytic TY model reaction of the substrate DTBP-H to the *o*-quinone DTBQ and the unphysiological side product 3,3′,5,5′-tetra-*tert*-butyl-2,2′-biphenol (CCcP).

mono- and dinucleating ligands developed by Casella *et al.*,[10] Stack *et al.*,[11] Ottenwaelder and Lumb *et al.*,[12] Herres-Pawlis *et al.*[13] and others.[2,5,6,14–21]

As the active site of TY contains two copper centres, dinucleating ligands have extensively been used to mimic TY activity.[2,4,8,15–18] Nevertheless, the number of dicopper(I) model systems supported by such ligands that exhibit catalytic tyrosinase activity has remained limited to date (Scheme 2). The first dinuclear system and also the first model for the monooxygenation of monophenols was reported by Bulkowski over 35 years ago.[19] In 1990, another dinuclear copper(I) complex based on the ligand **BiPh(impy)$_2$** was published by Réglier *et al.*,[20] mediating the catalytic conversion of the model

[a] *R. Schneider, Dr. T. A. Engesser, Dr. J. N. Hamann, Prof. Dr. C. Näther, Prof. Dr. F. Tuczek*
Institute of Inorganic Chemistry
Christian-Albrechts-University of Kiel
Max-Eyth-Straße 2, 24118 Kiel, Germany
E-mail: ftuczek@ac.uni-kiel.de

Supporting information for this article is available on the WWW under https://doi.org/10.1002/ejic.202200509

Research Article
doi.org/10.1002/ejic.202200509

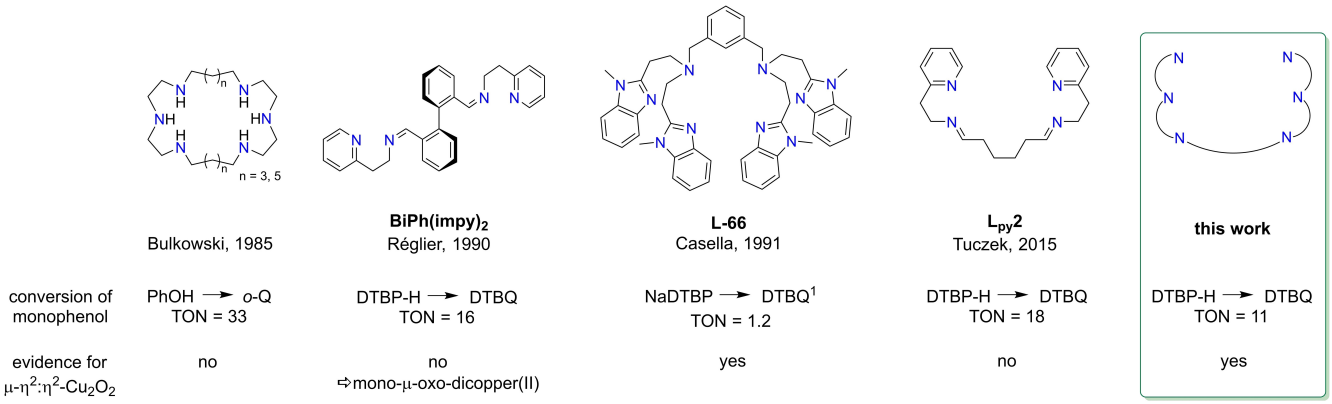

Scheme 2. Dinucleating ligands used in small molecule model systems for tyrosinase-like oxygenation reactions.[19–24] The conversion of monophenol was carried out under *Bulkowski-Réglier-conditions*,[19,20] the TON (turnover number) refers to one dicopper unit. [1] Sodium di-*tert*-butylphenolate (1.5 eq.) was oxygenated in the presence of dicopper(I) catalyst in acetonitrile.[23]

substrate 2,4-di-*tert*-butylphenol (DTBP-H) to 3,5-di-*tert*-butylquinone (DTBQ) (Scheme 1b). However, the active μ-η^2:η^2-peroxo-dicopper(II) species being responsible for the reactivity of the enzyme was not observed with these systems. The Cu_2**L-66**-system developed by Casella *et al.*, on the other hand, does form this intermediate upon reaction with dioxygen, as evidenced by use of low temperature UV/vis and resonance Raman spectroscopy.[22–24] Moreover, a correlation between the μ-η^2:η^2-peroxo-dicopper(II) species and the stoichiometric hydroxylation of 4-methoxyphenol to the corresponding catechol as well as the oxidation of 3,5-di-*tert*-butylcatechol to DTBQ was demonstrated,[22–24] establishing this system as a true tyrosinase mimic. Nevertheless, only a slightly over-stoichiometric conversion of a monophenolate to the corresponding *o*-quinone has been evidenced for this system.[22–24] This appears to conform to a more general trend; i.e. no copper complex supported by a dinucleating ligand has been reported to date that both forms a stable μ-η^2:η^2-peroxo-dicopper(II) species and catalytically converts phenols to *o*-quinones (cf. Scheme 2). In 2015, with the aim of filling this gap, we synthesized the dinucleating ligand $\mathbf{L_{py}2}$ derived from its mononucleating counterpart $\mathbf{L_{py}1}$[25] and examined the reactivity of the derived copper(I) complex. Whereas a catalytic conversion of DTBP-H to DTBQ could be observed, no copper-oxygen species was detectable.[21] Therefore, in a new attempt towards this goal, we herein present a modified ligand design that is based on previous mononuclear systems[21,26] and the known dinuclear models.[20–22,24] In order to stabilize a μ-η^2:η^2-peroxo intermediate, we now employ a bis-tridentate structure. Based on earlier catalytically active TY models supported by ligands with imine donors (see above), we further decided to include such groups in our ligands. However, for comparison, we also wanted to study analogous ligands with amine groups. Finally, to avoid ligand hydroxylation that often occurs in dinuclear complexes supported by dinucleating ligands,[27] an alkyl chain is employed as a spacer between the two tridentate side arms. In contrast to other known bis-tridentate *N*-donor ligands which are alkyl bridged via the central *N*-donors,[28] here the bridging occurs via the terminal *N*-donors for which pyrazole moieties were selected due to their favourable properties in TY model chemistry.[2,6] All in all, it is expected that the resulting scaffolds enable formation of Cu_2O_2-intermediates as well as mediate tyrosinase-like activity. In the following, the synthesis of the described ligands and their corresponding dicopper(I) complexes (Scheme 3) is presented, as well as the results of low temperature UV/vis-experiments and oxygenation reactions with DTBP-H as substrate.

Results and Discussion

The symmetric bis-tridentate ligands $\mathbf{L^{MO4}}$ (**1a**) and $\mathbf{L^{MO5}}$ (**1b**) were synthesized in two steps starting from 3-formyl-1*H*-pyrazole (**7**), which was synthesized by slight modification of the literature.[29] In the penultimate reaction step, two equivalents of **7** were linked by *N*-alkylation following the prescription of Bol *et al.*[30] This is the limiting reaction step, as only moderate yields (29% for **8a**, 23% for **8b**) could be obtained. Nevertheless, the target ligands could be synthesized in the subsequent final step. For this purpose, 1,4-bis(3-formyl-1*H*-pyrazol-1-yl)butane (**8a**) or 1,5-bis(3-formyl-1*H*-pyrazol-1-yl)pentane (**8b**) was reacted with 2-(2-pyridyl)ethylamine in a reductive amination according the procedure published by Bol *et al.*[30] The amines **1a** and **1b** were isolated by aqueous workup as viscous oils (92% resp. 47%), which were dried in vacuo. Despite extensive efforts, traces of water could not be removed. The imine ligands $\mathbf{L^{MO4im}}$ (**2a**) and $\mathbf{L^{MO5im}}$ (**2b**), on the other hand, were obtained by imine condensation of the dialdehyde **8a** resp. **8b** with 2-(2-pyridyl)ethylamine. The reaction was performed in toluene and in the presence of molecular sieve (3 Å), preventing hydrolysis of the imine formed. After a reaction time of 18 h at room temperature and removal of both the molecular sieve and the solvent, the target ligands $\mathbf{L^{MO4im}}$ (**2a**) and $\mathbf{L^{MO5im}}$ (**2b**) were obtained in good purities and yields (91% resp. 93%).

Research Article
doi.org/10.1002/ejic.202200509

Chemistry Europe
European Chemical Societies Publishing

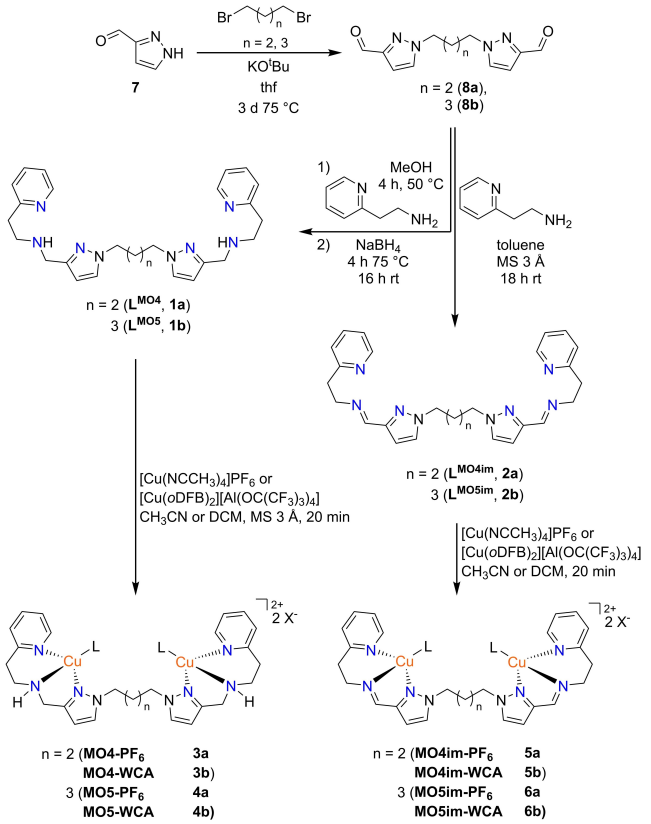

Scheme 3. Reaction scheme of the synthesis of the ligands $\mathbf{L^{MO4}}$ (**1a**), $\mathbf{L^{MO5}}$ (**1b**), $\mathbf{L^{MO4im}}$ (**2a**) and $\mathbf{L^{MO5im}}$ (**2b**) and their corresponding dicopper(I) complexes (L = $NCCH_3$ for **3**–**6a**, **3**–**6b** don't have additional ligands; X = PF_6^-, $[Al(OC(CF_3)_3)_4]^-$ ≡ WCA).

In order to synthesize dicopper(I) complexes supported by the amine ligands $\mathbf{L^{MO4}}$ (**1a**) and $\mathbf{L^{MO5}}$ (**1b**), the freshly dried ligands were each dissolved in either acetonitrile or dichloromethane and added to a solution of two equivalents of copper(I) precursor ($[Cu(NCCH_3)_4]PF_6$ or $[Cu(oDFB)_2]$WCA with *o*DFB = *ortho*-difluorobenzene and WCA = $[Al(OC(CF_3)_3)_4]^-$).[31] Unfortunately, isolation of the target compounds in solid form was not possible. NMR-spectroscopic analysis of a freshly prepared solution of ligand ($\mathbf{L^{MO4}}$ resp. $\mathbf{L^{MO5}}$) and the copper(I) precursor, on the other hand, showed that the complexes **MO4-X** (X = PF_6^- **3a**) and **MO5-X** (X = PF_6^- **4a**) can be generated *in situ* (Figure S6 and Figure S7). In contrast, complexation reactions with the imine ligands **2a**/**2b** according to the described procedure gave access to the desired dicopper(I) complexes **MO4im-X** (X = PF_6^- **5a**, X = WCA^- **5b**) and **MO5im-X** (X = PF_6^- **6a**, X = WCA^- **6b**) (Scheme 3) as crystalline solids. The NMR spectroscopic analysis of these solids prove the formation of diamagnetic compounds with different chemical shifts for the ligand signals in the ^{1}H-NMR spectra compared to the pure ligands. Furthermore, high resolution mass spectra were obtained for the dicopper(I) complexes of **MO4im-PF$_6$** (**5a**) and **MO5im-PF$_6$** (**6a**). Due to the aluminate as anion, a mass spectrometric analysis of **5b** and **6b** is not possible.

Determination of the molecular structure of crystals grown from a solution of **MO4im-PF$_6$** (**5a**) in a mixture of acetonitrile (< 1 %) and 2-methyltetrahydrofuran showed the expected coordination geometry of the two copper(I) centres (Figure 1, for more details see SI). Each of them is bound to the three *N*-donors of the tridentate side arms of the ligand as well as one acetonitrile coligand in a tetrahedrally-distorted geometry. Compound **5a** crystallizes in the triclinic space-group *P-1* with one unit per unit cell. The bond angles within the chelating side arm are N_{pz}-Cu-N_{imin} 78.25(6)° and N_{py}-Cu-N_{imin} 89.01(6)°. The average metal-ligand bond length is 2.045 Å. The two copper centres are rotated away from each other, which is made possible by the high flexibility of the ligand backbone.

In order to study the formation of copper-oxygen species, low-temperature UV/vis-spectroscopy was employed, using *in situ* generated Cu(I) complexes. With the copper(I) complexes **5b** and **6b** derived from the imine-containing ligands **2a** and **2b**, resp., and WCA as anion the emergence of an absorption band at 364 nm was observed at low temperatures (163–173 K in 2-methyltetrahydrofuran), indicating formation of a μ-η^2:η^2-peroxo-dicopper(II) species (Figure 2 and Figures S20 for **5b**, S21 for **6b**).

The UV/vis spectra obtained upon oxygenation of **MO4im-WCA** (**5b**, 60 µm) at 163 K show that the intensity of the absorption band at 364 nm continuously increases upon exposure to dioxygen, reaching a maximum absorbance of 0.17 (Figure 2). The comparison with the literature-known μ-η^2:η^2-peroxo-dicopper intermediates[4,7,24,32] suggests that such a species has formed. In general, the peroxo → Cu(II) LMCT band of μ-η^2:η^2-peroxo-dicopper complexes have molar decadic absorption coefficients of about 20000 $M^{-1}cm^{-1}$.[4,7,32,33] Compared to this value, the absorbance obtained upon oxygenation of **MO4im-WCA** (**5b**) corresponds to a peroxo formation of 14 %. For **MO5im-WCA** (**6b**) a maximum absorbance of 0.26 (23 %) was obtained (Figure S21). Upon heating to room temperature the intensity of the 364 nm band vanishes, but the initial Cu(I)-spectrum is not recovered (cf. Figures S20, S21). This is compatible with irreversible decay of the peroxo complex.

The relatively low yields of the peroxo intermediates observed for **5b** and **6b** indicate an incomplete formation of the peroxo complex, which suggests a limited stability of this species. Nevertheless, it can be stated that the imine-systems **MO4im-** and **MO5im-WCA** (**5b**/**6b**) are able to form, at least in part, the same Cu_2O_2 species which is responsible for the

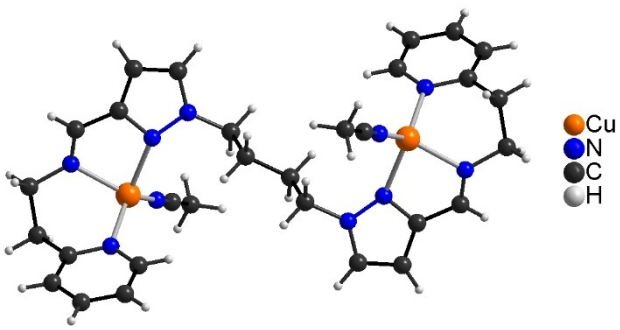

Figure 1. Molecular structure of **MO4im-PF$_6$** (**5a**), PF_6^- anions are omitted for clarity.

Research Article
doi.org/10.1002/ejic.202200509

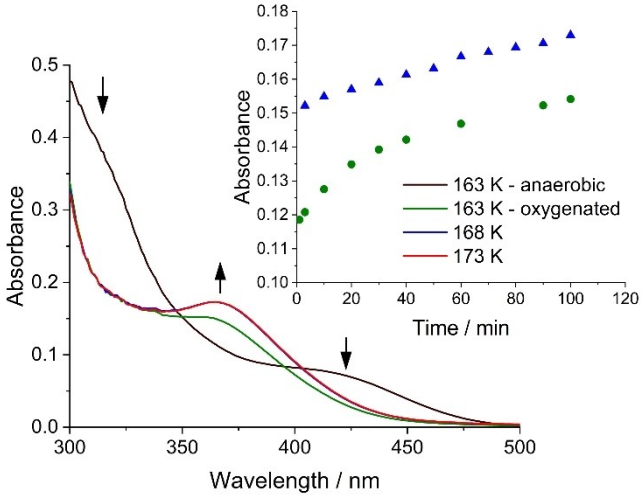

Figure 2. UV/vis spectra obtained upon oxygenation of a solution of **MO4im-WCA** (**5 b**, 60 μM, *in situ* generated) in 2-methyltetrahydrofuran at low temperatures and subsequent gradual heating, quartz cell length l = 1 cm. Inset: Absorbance at 364 nm and 163 K (green dots) resp. 168 K (blue triangles) after oxygenation as function of time.

monooxygenase activity of the enzyme TY and thus might also be able to perform the tyrosinase-like conversion of DTBP-H to DTBQ (see below). On the other hand, UV/vis-spectroscopic measurements performed under the same conditions with the dicopper(I) complexes **3 b** and **4 b** derived from the amine-containing ligands **1 a** and **1 b**, resp., showed a much weaker intensity of the 364 nm band (Figure S17, Figure S18). This suggests an even lower stability of the μ-η^2:η^2-peroxo complex as compared to the imine-based systems.

Having examined the possible formation of dioxygen adducts, oxygenation reactions with the Cu(I) complexes supported by the four bis-tridentate ligands $\mathbf{L^{MO4}}$/$\mathbf{L^{MO5}}$ (**1 a**/**1 b**) and $\mathbf{L^{MO4im}}$/$\mathbf{L^{MO5im}}$ (**2 a**/**2 b**) were carried out. The tyrosinase-like oxygenation reaction was performed under *Bulkowski-Réglier-conditions*[19,20] with DTBP-H as substrate, using *in situ* generated Cu(I) complexes. Accordingly, oxygen was added to a solution of the dinucleating ligand (250 μM), Cu(I) precursor ([Cu(NCCH$_3$)$_4$]PF$_6$, 500 μM), substrate (DTBP-H, 25 mM), and base (NEt$_3$, 50 mM). The effect of triethylamine on the reactivity of copper complexes towards the monooxygenation of 2,4-di-*tert*-butylphenol has also been emphasized by Lumb *et al.*[34] The reaction was monitored by UV/vis spectroscopy for 2 h and subsequently quenched by addition of 6 M hydrochloric acid. The organic reaction products were analyzed by NMR spectroscopy. Importantly, no formation of DTBQ could be observed using the amine-systems (**MO4-** and **MO5-PF$_6$**, **3 a**/**4 a**) as catalysts (Figure 3, left for **MO4-PF$_6$** (**3 a**) and Figure S23 for **MO5-PF$_6$** (**4 a**)). Instead of DTBQ, only the C–C-coupling product 3,3′,5,5′-tetra-*tert*-butyl-2,2′-biphenol (CCcP) was detected (Figure S22, Figure S24, cf. Table 1). These findings correspond to results obtained with the dinuclear Cu$_2$**L-66**-system[22,23] and the mononuclear complex Cu(**pzea**)PF$_6$ supported by the ligand bis[2-(1*H*-pyrazol-1-yl)ethyl]amine,[35] both of which only mediate a slightly over-stoichiometric conversion of DTBP-H to DTBQ.

Analogous experiments were performed using the imine systems **MO4im-PF$_6$** (**5 a**) and **MO5im-PF$_6$** (**6 a**) as catalysts. Additionally, the isolated **MO4im**-complexes with PF_6^- as well as WCA^- as anion were used in order to check whether it makes a difference which anion is employed and whether the reaction is carried out with the isolated or the complex formed *in situ* (Table S6). Notably, **MO4im-PF$_6$** (**5 a**) and **MO4im-WCA** (**5 b**) were found to be almost inactive towards the monooxygenation of DTBP-H. The formation of the characteristic absorption band of DTBQ at 405 nm could be observed during the first 5 minutes of the reaction, corresponding to a yield of DTBQ of 5 %. However, the intensity of this band did not increase in the further course of the reaction. Moreover, the NMR spectroscopic analysis of the reaction product showed a high yield of the

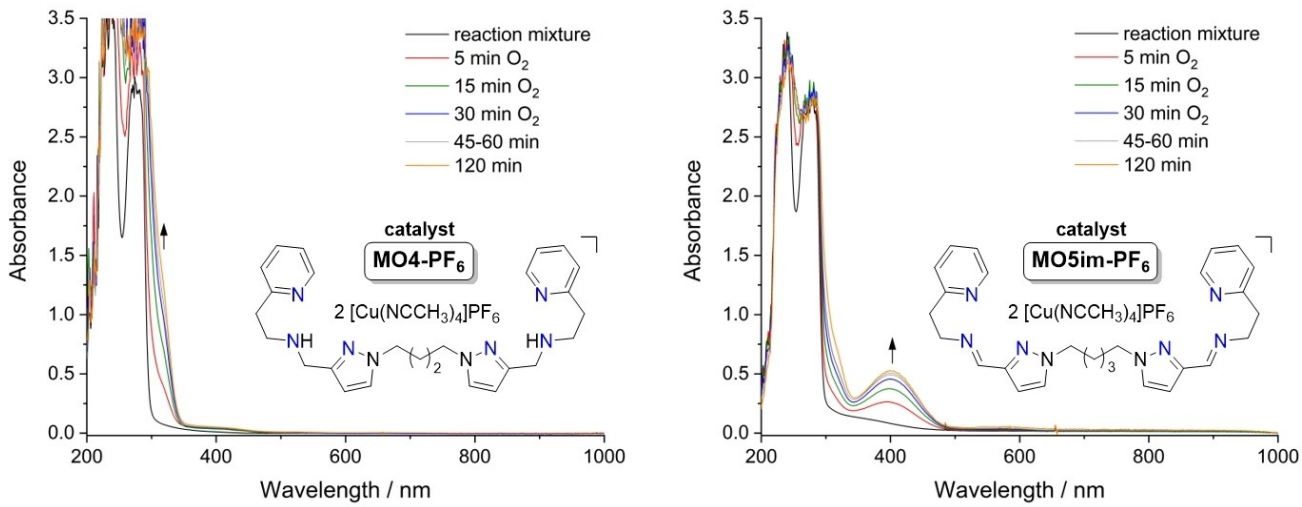

Figure 3. UV/vis spectra measured during the oxygenation reaction of DTBP-H (25 mM) in the presence of NEt$_3$ (50 mM) and **MO4-PF$_6$** (**3 a**, 250 μM, left) resp. **MO5im-PF$_6$** (**6 a**, 250 μM, right) as catalyst in dichloromethane for the first 2 h, quartz cell length l = 0.1 cm.

Research Article
doi.org/10.1002/ejic.202200509

Table 1. Activities for the tyrosinase-like oxygenation of DTBP-H[a] mediated by the model systems **MO4-PF$_6$**, **MO5-PF$_6$**, **MO4im-PF$_6$**, **MO5im-PF$_6$**.

yield/% (h)[b]	MO4-PF$_6$ 0 (2)	MO4im-PF$_6$ 5 (2)	MO5-PF$_6$ 0 (2)	MO5im-PF$_6$ 11 (2)
reaction rate[c]/ 10^{-4} Mmin^{-1}				
0–5 min	–	1.91 ± 0.13	–	2.81 ± 0.17
0–15 min	–	0.75 ± 0.03	–	1.35 ± 0.04
0–30 min	–	0.41 ± 0.01	–	0.83 ± 0.02
product ratio[d]	64:0:36	57:3:40	39:0:61	82:8:10

[a] The tyrosinase-like reaction was carried out under *Bulkowski-Réglier-conditions*[19,20] by injection of oxygen in a solution of the dicopper(I) catalyst (250 μM), DTBP-H (25 mM) and NEt_3 (50 mM) in dichloromethane. [b] The yield with respect to the used substrate quantity was determined via UV/vis spectroscopy. [c] The reaction rate was calculated by dividing the product concentration calculated from the UV/vis spectra by the reaction time. [d] The ratio of the reaction products (DTBP-H:DTBQ:CCcP) was calculated from the ^{1}H-NMR spectra.

coupling product CCcP (40%). In contrast, catalytic monooxygenase activity (11% DTBQ) was observed with **MO5im-PF6** (**6a**) as catalyst (Figure 3 <xfigr3> right, cf. Table 1) whereby only 10% CCcP were formed.

To sum up, it is found that the dicopper(I) complexes **MO4-** and **MO5-PF$_6$** (**3a**/**4a**) supported by the amine-containing ligands **1a** and **1b** do not catalyze the monooxygenation of DTBP-H. Instead, they only form the C–C coupling product CCcP whereas their analogues **MO4im-PF$_6$** and **MO5im-PF$_6$** (**5a**/**6a**) supported by the imine-containing ligands **2a** and **2b** mediate the catalytic conversion of DTBP-H to DTBQ, the catalyst with a C5-bridge being about twice as active as its counterpart bridged by a C4-chain.

Several factors may be invoked to explain these striking structure-reactivity correlations. First of all, the monooxygenation activity could critically depend on the formation of the μ-η^2:η^2-peroxo intermediate, which is found to an increasing extent in the series **MO4**/**MO5** ≪ **MO4im** < **MO5im** (see above). However, a more stable μ-η^2:η^2-peroxo intermediate may be *less* reactive towards the oxygenation of phenolic substrates.[6] It is therefore of interest to consider the influence of the amine vs. the imine donors on the reactivity of this intermediate in more detail. In principle this influence can derive from electronic or structural factors. In terms of the former, the weaker donating imine function could result in an increased electrophilicity of the peroxo unit compared to the amine donors and thus lead to an increased reactivity towards the hydroxylation of aromatic substrates. In terms of geometrical parameters, replacing amine by imine groups causes a reduced flexibility of the ligand framework which may lead to a distorted coordination geometry, possibly increasing the probability for binding of a substrate.

To obtain further insight into these points, DFT geometry optimizations were performed for the μ-η^2:η^2-peroxo-dicopper(II) intermediates of our complexes. Notably, the charges on the oxygen atoms of the peroxo moiety were found to be in the same range for all systems, giving no indication of an increased electrophilicity in the imine systems (Table S3). In contrast, the geometry-optimized structures showed significant differences due to the rigidity of the imine functions.[36] Specifically, the amine-based systems **MO4** and **MO5** exhibit almost planar μ-$\eta 2$:$\eta 2$- peroxo-dicopper(II)-units with typical Cu–Cu distances of 3.62 Å resp. 3.63 Å (Figure 4a for **MO5**, Figure S15a for **MO4**),[32] whereas for imine-based complexes **MO4im** and **MO5im** optimization of the μ-η^2:η^2-peroxo intermediates leads to butterfly-distorted structures with Cu–Cu-distances of 3.43 Å resp. 3.40 Å (Figure 4b for **MO5im**, Figure S15b for **MO4im**). Moreover, both in **MO4** and **MO5**, the copper centres are coordinated in an approximate square-pyramidal fashion where the pyridine *N*-donors as well as the amine donors are in a plane with the peroxo unit and the pyrazole *N*-donors coordinate axially. In contrast, the rigidity of the imine function causes the pyridine ligands being no longer in a plane with the peroxo unit and the imine donors, and the corresponding complexes exhibit a geometry between square-pyramidal and trigonal-bipyramidal. This opens up an equatorial position where the substrate (a phenolate) can attack. Notably, bonding of the substrate within the plane of the peroxo core, causing overlap between the σ* orbital of the peroxide and the π orbital of the arene ring, has been formulated as a precondition for the aromatic hydroxylation of phenols mediated by side-on peroxo-bridged dicopper cores.[5]

The structural distortion caused by the imine function is more pronounced in **MO5im** than in **MO4im**, in line with the increased activity of the former system. On the other hand, the absence of free equatorial positions in the amine systems **MO4** and **MO5** hinders attack of phenolic substrate and, conse-

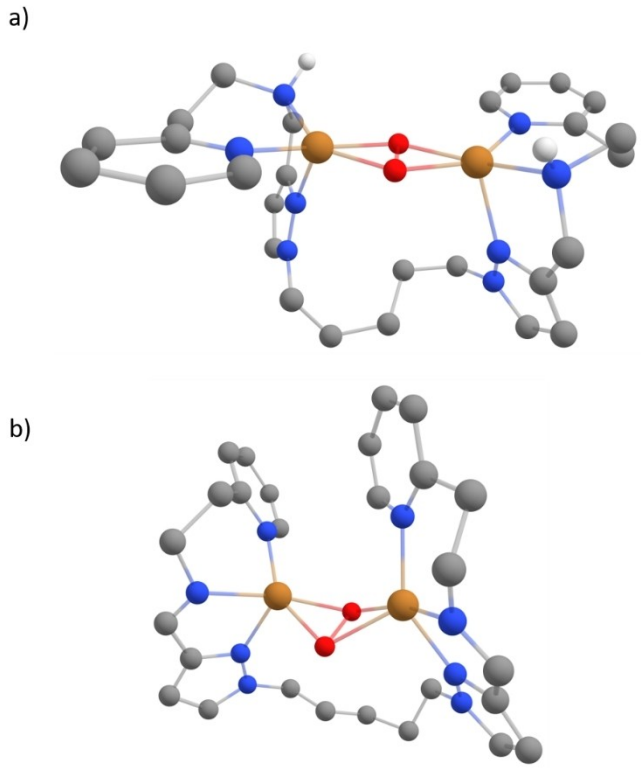

Figure 4. Optimized structures of the μ-η^2:η^2-peroxo-dicopper(II)-complexes expected to form upon reaction of **MO5** (a) and **MO5im** (b) with dioxygen.

Research Article
doi.org/10.1002/ejic.202200509

quently, their monooxygenation. This causes side reactions such as C–C coupling, explaining the high value of CCcP formation found for the latter systems. Notably, these reactions are initiated by electron transfer from the phenolate to the μ-peroxo intermediate, generating phenoxyl radicals,[6,37] which is mechanistically less demanding than the monooxygenation pathway and thus is preferred if the latter is hindered for steric reasons.

Recently, we have shown that the tyrosinase-like monooxygenation of phenols mediated by copper-containing small-molecule model systems can also follow a mononuclear mechanism,[14] besides the classic dinuclear pathway. Since reaction of the dicopper(I) complexes with dioxygen was only investigated at low-temperatures and the intensity of the μ-η^2:η^2-peroxo→Cu(II) CT band was found to be weak (see above), it is *a priori* not clear whether dinuclear copper-oxygen species also form under catalytic conditions (i.e., in dichloromethane, at room temperature and in the presence of substrate and base) and whether these species in fact mediate conversion of the monophenols to the *o*-quinones. In order to address this issue, kinetic studies with **MO5im-PF$_6$** (**6a**) were conducted. The reaction rate of the formation of DTBQ was found to be linearly dependent on the concentration of the dinuclear copper(I) catalyst used (Figure 5, cf. Figure S35). Thus, the rate-limiting step of the mechanism includes an intramolecularly formed, dinuclear copper-oxygen species (for more details see SI), in line with the classical tyrosinase mechanism.[5–7]

Conclusion

In summary, four bis-tridentate *N*-donor ligands were synthesized and their corresponding dicopper(I) complexes were investigated regarding their ability to form a Cu_2O_2-intermediate and to mediate the conversion of DTBP-H to DTBQ. For the imine complexes **MO4im** and **MO5im**, μ-η^2:η^2-peroxo-dicopper(II) species could be detected by UV/vis spectroscopy at low temperatures. Furthermore, these systems exhibit catalytic monooxygenase activity. In contrast, the amine-based model complexes **MO4-X** and **MO5-X** (X = PF_6^-, WCA^-) are inactive. The increased activity in the series **MO4**/**MO5** < **MO4im** < **MO5im** can be attributed to the degree of geometrical distortion in the corresponding DFT-optimized μ-η^2:η^2-peroxo-dicopper(II) structures. This distortion opens up an equatorial position allowing substrate bonding, which is essential for the hydroxylation reaction.[5] Furthermore, the involvement of an intramolecularly formed, dinuclear species in the rate-determining reaction step was proven by kinetic investigations. Thus, the imine system **MO5im-PF$_6$** represents the first model complex supported by a dinucleating ligand, that both forms a μ-η^2:η^2-peroxo-dicopper(II) intermediate and exhibits catalytic tyrosinase-like activity with DTBP-H as substrate via a dinuclear copper-oxygen intermediate.

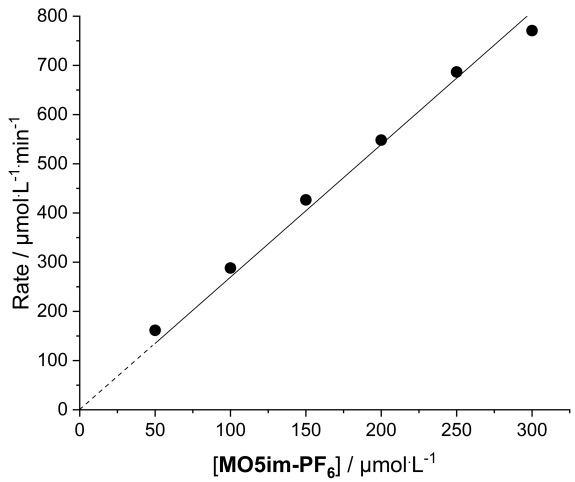

Figure 5. Dependence of the reaction rate (0–1 min) of the formation of DTBQ on the concentration of **MO5im-PF$_6$** (**6a**, *in situ* generated) = 50-300 µM, c(DTBP-H) = 25 mM, c(NEt_3) = 50 mM.

Experimental Section

Materials and Methods: The commercial available starting materials were purchased from Sigma Aldrich, ABCR, TCI chemicals or Fluorochem in reagent grade. Unless otherwise noted, these reagents were used without further purification. Oxygen- and/or moisture-sensitive materials, especially all copper(I) complexes, were handled using standard Schlenk techniques (nitrogen atmosphere dried over granulate P_4O_{10}) and a MBraun LABmaster glove box filled with nitrogen (O_2 < 1 ppm and H_2O < 1 ppm). All solvents were of commercially available reagent grade. Acetonitrile, dichloromethane, toluene and triethylamine were dried by heating to reflux under nitrogen or argon atmosphere over calcium hydride, methanol was dried analogously over magnesium, tetrahydrofuran over potassium. Anhydrous deuterated solvents were freeze-pump-thaw degassed and dried over 4 Å molecular sieves. [Cu(*o*DFB)$_2$][Al(OC(CF_3)$_3$)$_4$] and 3-Hydroxymethyl-1*H*-pyrazole were synthesized according to the published procedure.[14,38] UV/Vis spectra were recorded at room temperature with an Agilent 8435 Technologies photodiode array spectrophotometer and a quartz cell with length l = 0.1 cm. Low-temperature measurements were performed with an Agilent Cary 5000 spectral photometer using a CryoVAC KONTI cryostat and a quartz cell with length l = 1.0 cm. NMR spectra were recorded at 300 K by use of either a Bruker AVANCE III HD Pulse Fourier Transform spectrometer operating at frequencies of 400.1 MHz (^{1}H-NMR), 100.6 MHz (^{13}C-NMR), 104.3 MHz (^{27}Al-NMR) and 376.5 MHz (^{19}F-NMR) or a Bruker AvanceNeo 500 operating at frequencies of 500.1 MHz (^{1}H-NMR) and 125.8 MHz (^{13}C-NMR). Referencing was performed using the solvent residue signal. Signals were assigned with the help of DEPT-135 and two-dimensional correlation spectra (^{1}H,^{1}H-COSY, ^{1}H,^{13}C-HSQC, ^{1}H,^{13}C-HMBC). Infrared spectra were recorded at room temperature on a Bruker Alpha FT-IR Spectrum with Platinum ATR setup or on a Bruker Vertex70 FT-IR spectrometer using a broadband spectral range extension VERTEX FM for full mid and far IR in the range of 6.000-80 cm^{-1}. Raman spectra were recorded at RT on a Bruker RAM II FT-Raman spectrometer using a liquid nitrogen cooled, highly sensitive Ge detector, 1064 nm radiation and 3 cm^{-1} resolution. Flash Column chromatography was carried out with a Biotage Isolera One Spectra with UV detector (λ = 200–400 nm) and prepacked SNAP Ultra cartridges (different size). R_f-values were determined by thin-layer chromatography on Polygram Sil G/UV254 (Macherey-Nagel, 0.2 mm particle size) with a Comag UV lamp (λ = 254 nm). The elemental analyses were performed using a Elementar Vario MICRO

Research Article
doi.org/10.1002/ejic.202200509

cube element analyzer; the samples were prepared in tin vessels and were burnt in a stream of oxygen. High-resolution ESI mass spectra (HR-ESI) were measured with a Thermo Scientific Q Exactive Plus.

Single Crystal Structure Determination: Data collection was performed with a XtaLAB Synergy, Dualflex, HyPix diffractometer using CuKα radiation (λ = 1.54184). The structure was solved with SHELXT[39] using Intrinsic Phasing and refined with SHELXL[40] using Least Squares minimisation. All non-hydrogen atoms were refined anisotropic. The C–H H atoms were positioned with idealized geometry and were refined isotropic with $U_{iso}(H) = 1.2\ U_{eq}(C)$. The tetrafluoro phosphate anion is disordered over two orientations and was refined using a split model with restraints for the geometry and the components of the anisotropic displacement parameters. Selected crystal data and details of the structure refinements can be found in Table S1, selected bond length are listed in Table S2 and an Ortep plot is presented in Figure S14.

Computational Details: DFT calculations were performed with ORCA 4.2.1.[41] The geometries of the dinuclear peroxo species were optimized by using the B3LYP functional[42] and the Ahlrichs def2-TZVP basis set[43] in conjunction with the chain of spheres approximation (RIJCOSX)[44] and the general Ahlrichs Coulomb fitting basis set denoted def2/J.[45] To account for dispersion effects Grimme's semiempirical dispersion correction scheme with Becke-Johnson damping (D3BJ)[46] was used. The antiferromagnetic coupling between the copper centres was included via a broken symmetry wave function with one unpaired electron on each copper ion.

General procedure for the oxygenation of 2,4-di-*tert*-butylphenol to mimic tyrosinase activity: To a solution of the ligand in dichloromethane (5 mM, 1 mL) was added a solution of the respective copper(I) precursor in dichloromethane (10 mM, 1 mL) under inert atmosphere. The complex mixture (2 mL) was diluted with a solution of 2,4-di-*tert*-butylphenol (100 eq.) in dichloromethane (3 mL) and 15 mL dichloromethane to afford a 250 μM solution of the model system. After addition of triethylamine (200 eq.) dioxygen was injected into the reaction mixture. The conversion of the substrate to 3,5-di-*tert*-butyl-*o*-quinone was monitored via UV/Vis and NMR spectroscopy.

General procedure for low temperature UV/vis spectroscopic measurements: To a solution of the ligand in a mixture of dichloromethane (< 3 %) and 2-methyltetrahydrofuran was added a solution of the respective copper(I) precursor (2 eq.) in 2-methyltetrahydrofuran under inert atmosphere. This solution was cooled under inert atmosphere and subsequently oxygenated. UV/vis spectra were recorded during injection of oxygen and upon gradual heating of the solution.

General procedure for kinetic measurements: To a solution of $\mathbf{L^{MO5im}}$ (**2b**) in dichloromethane (5 mM, 6 mL) was added a solution of $[Cu(NCCH_3)_4]PF_6$ in dichloromethane (10 mM, 6 mL) under inert atmosphere. Additionally, a solution of DTBP-H (516 mg, 2.50 mmol) and NEt_3 (700 μL, 5.02 mmol) in oxygen-saturated dichloromethane (79.3 mL) was prepared. For each copper(I) concentration examined, 8 mL of the latter solution were mixed with complex solution and filled up to a total volume of 10 mL with absolute dichloromethane. The reaction progress was determined by UV/vis-spectroscopy in one-minute intervals over 5 minutes, starting after one minute of reaction time.

Synthesis

3-Formyl-1*H*-pyrazole (7): Compound **7** was synthesized according to the literature.[29] The published procedure was slightly modified. Activated manganese(IV) oxide (8.02 g, 92.2 mmol) was added to a solution of 3-Hydroxymethyl-1*H*-pyrazole (1.50 g, 15.3 mmol) in 80 mL ethyl acetate. The mixture was heated to reflux for 4 h and subsequently cooled to room temperature. The solids were removed by filtration over celite. The filtrate was concentrated in vacuo and the residue washed with methanol to afford compound **7** as off-white powder (908 mg, 9.45 mmol, 62 %). ^{1}H NMR (400.1 MHz, $SO(CD_3)_2$): δ = 13.73 (br s, N*H*), 9.93 (s, 1H, C_{pz}-*CH*O), 7.93 (d, ^3J = 2.1 Hz, 1H, C_{pz}-*H5*), 6.77 (d, ^3J = 2.3 Hz, 1H, C_{pz}-*H4*) ppm; ^{13}C NMR (100.6 MHz, $SO(CD_3)_2$): δ = 187.1 (C_{pz}-CHO), 151.3 (C_{pz}3), 130.9 (C_{pz}5), 104.3 (C_{pz}4) ppm; elemental analysis calcd (%) for $C_4H_4N_2O$: C 50.00, H 4.20, N 29.15; found: C 50.00, H 4.31, N 29.08.

1,4-Di-(3-formyl-1*H*-pyrazol-1-yl)butane (8a): Compound **7** (483 mg, 5.03 mmol) was dissolved in 20 mL tetrahydrofuran by refluxing for 1 h and afterwards cooled in an ice bath. After addition of 1,4-dibromobutane (290 μL, 2.46 mmol), potassium *tert*-butoxide (564 mg, 5.03 mmol) was added in small portions. The reaction mixture was first allowed to warm to room temperature and then heated to 75 °C for 3 days. After cooling to room temperature, the solvent was evaporated under reduced pressure. The residue was dissolved in dcm and the organic layer washed with water. The organic layer was dried with sodium sulfate and the solvent evaporated under reduced pressure. The crude product was purified by column chromatography on silica gel (TLC: cyclohexane/ethyl acetate 1:4, R_f = 0.29) to obtain the desired product as a colourless oil that crystalizes slowly (178 mg, 723 μmol, 29 %). ^{1}H NMR (500.1 MHz, $CDCl_3$): δ = 9.93 (d, ^5J = 0.5 Hz, 2H, C_{pz}-*CH*O), 7.41 (dd, ^5J = 0.7 Hz, ^3J = 2.4 Hz, 2H, C_{pz}-*H5*), 6.78 (d, ^3J = 2.4 Hz, 2H, C_{pz}-*H4*), 4.25-4.18 (m, 4H, $N_{pz}CH_2(CH_2)_2CH_2N_{pz}$), 1.96-1.89 (m, 4H, $N_{pz}CH_2(CH_2)_2CH_2N_{pz}$) ppm; ^{13}C NMR (125.8 MHz, $CDCl_3$): δ = 186.4 (C_{pz}-CHO), 151.7 (C_{pz}3), 131.3 (C_{pz}5), 106.3 (C_{pz}4), 52.3 ($N_{pz}CH_2(CH_2)_2CH_2N_{pz}$), 27.3 ($N_{pz}CH_2(CH_2)_2CH_2N_{pz}$) ppm; IR (neat): 3349 (vw), 3146 (vw), 2950 (w), 2875 (vw), 2839 (w), 2787 (w), 1722 (w), 1682 (vs), 1638 (s), 1511 (w), 1479 (s), 1466 (s), 1447 (s), 1403 (s), 1379 (w), 1331 (s), 1319 (s), 1275 (s), 1247 (w), 1203 (vs), 1143 (s), 1103 (w), 1060 (vs), 1024 (w), 1003 (s), 864 (w), 756 (vs), 672 (w), 629 (s), 521 (vw), 437 (s) cm^{-1}; HRMS (ESI): *m/z* calcd for $C_{12}H_{14}N_4O_2 + H^+$: 247.11895 $[M+H]^+$; found: 247.11875; elemental analysis calcd (%) for $C_{12}H_{14}N_4O_2$: C 58.53, H 5.73, N 22.75; found: C 58.38, H 5.77, N 22.27.

1,5-Di-(3-formyl-1*H*-pyrazol-1-yl)pentane (8b): Compound **8b** was synthesized according to the procedure described for compound **8a**. Instead of 1,4-dibromobutane, 1,5-dibromopentane (320 μL, 2.37 mmol) was used, TLC: cyclohexane/ethyl acetate 1:4, R_f = 0.45. The desired product was obtained as colourless oil that crystalizes slowly (151 mg, 580 μmol, 23 %). ^{1}H NMR (500.1 MHz, $CDCl_3$): δ = 9.95 (d, ^5J = 0.7 Hz, 2H, C_{pz}-*CH*O), 7.40 (dd, ^5J = 0.8 Hz, ^3J = 2.4 Hz, 2H, C_{pz}-*H5*), 6.79 (d, ^3J = 2.4 Hz, 2H, C_{pz}-*H4*), 4.20 (t, ^3J = 7.0 Hz, 4H, ($N_{pz}CH_2CH_2)_2CH_2$), 2.05-1.85 (m, 4H, ($N_{pz}CH_2CH_2)_2CH_2$), 1.41-1.21 (m, 2H, ($N_{pz}CH_2CH_2)_2CH_2$) ppm; ^{13}C NMR (125.8 MHz, $CDCl_3$): δ = 186.4 (C_{pz}-CHO), 151.5 (C_{pz}-3), 131.3 (C_{pz}-5), 106.2 (C_{pz}-4), 52.7 ($N_{pz}CH_2CH_2)_2CH_2$), 29.7 ($N_{pz}CH_2CH_2)_2CH_2$), 23.5 ($N_{pz}CH_2CH_2)_2CH_2$) ppm; IR (neat): 3122 (w), 2942 (w), 2863 (w), 2826 (w), 2779 (vw), 1690 (vs), 1511 (w), 1503 (w), 1471 (s), 1442 (w), 1403 (s), 1363 (s), 1331 (s), 1315 (s), 1251 (s), 1203 (vs), 1155 (s), 1060 (s), 1003 (w), 992 (w), 936 (vw), 864 (w), 756 (vs), 672 (w), 629 (w), 556 (w) cm^{-1}; HRMS (ESI): *m/z* calcd for $C_{13}H_{16}N_4O_2 + H^+$: 261.13460 $[M+H]^+$; found: 261.13429.

1,4-Di-3-((1-(2-pyridylethyl)amino)methylene)-1*H*-pyrazol-1-yl)-butane (1a): Under inert atmosphere, 2-(2-pyridyl)ethylamine (190 μL, 1.14 mmol) was added to a solution of compound **8a** (158 mg, 642 μmol) in methanol (20 mL). The reaction mixture was stirred for 2 h at 50 °C. After cooling to room temperature, sodium borohydride (146 mg, 3.85 mmol) was added in small portions. The mixture was heated to reflux for 4 h and afterwards stirred at room

temperature for additional 16 h. The solvent was evaporated under reduced pressure and the residue was dissolved in water (15 mL) and acidified with conc. hydrochloric acid (pH 3). This layer was washed twice with dichloromethane and then alkalized with sodium carbonate (pH 11). The solution was extracted with dichloromethane (3-times). The combined organic layer were dried with sodium sulfate and concentrated in vacuo to afford compound **1a** as dark yellow, very viscous oil (271 mg, 591 μmol, 92%). ^{1}H NMR (500.1 MHz, $CDCl_3$): δ = 8.48 (dd, ^3J = 2.1 Hz, ^3J = 2.8 Hz, 2H, C_{py}-*H*6), 7.56 (tt, ^3J = 2.0 Hz, ^3J = 7.7 Hz, 2H, C_{py}-*H*4), 7.22 (d, ^3J = 2.1 Hz, 2H, C_{pz}-*H*5), 7.15 (d, ^3J = 7.8 Hz, 2H, C_{py}-*H*5), 7.11–7.07 (m, 2H, C_{py}-*H*3), 6.14 (d, ^3J = 2.1 Hz, 2H, C_{pz}-*H*4), 4.04–3.97 (m, 4H, $N_{pz}CH_2(CH_2)_2CH_2N_{pz}$), 3.83 (s, 4H, C_{pz}-CH_2NH_2), 3.09-3.03 (m, 4H, C_{py}-CH_2CH_2), 3.03-2.98 (m, 4H, C_{py}-CH_2CH_2), 2.79 (br s, N*H*), 2.74 (br s, N*H*), 1.82-1.73 (m, 4H, $N_{pz}CH_2(CH_2)_2CH_2N_{pz}$) ppm; ^{13}C NMR (125.8 MHz, $CDCl_3$): δ = 160.2 (C_{py}-2), 150.9 (C_{pz}-3), 149.3 (C_{py}-6), 136.5 (C_{py}-4), 130.0 (C_{pz}-5), 123.4 (C_{py}-3), 121.4 (C_{py}-5), 104.5 (C_{pz}-4), 51.5 ($N_{pz}CH_2(CH_2)_2CH_2N_{pz}$), 48.9 ($C_{py}$-$CH_2CH_2$), 47.0 ($C_{pz}$-$CH_2$NH), 38.0 ($C_{py}$-$CH_2CH_2$), 27.6 ($N_{pz}CH_2(CH_2)_2CH_2N_{pz}$) ppm; IR (neat): 3381 (br, s), 3273 (br, s), 3010 (vw), 2934 (s), 2826 (br, s), 1642 (br, w), 1586 (s), 1571 (s), 1514 (s), 1471 (s), 1431 (vs), 1366 (s), 1311 (s), 1208 (s), 1151 (w), 1103 (s), 1048 (s), 1000 (s), 845 (vw), 761 (br, vs), 629 (w), 609 (w), 513 (vw) cm^{-1}; HRMS (ESI): *m/z* calcd for $C_{26}H_{34}N_8 + H^+$: 459.29792 $[M+H]^+$; found: 459.29685, elemental analysis calcd (%) for $C_{26}H_{34}N_8 \cdot 1.5H_2O$: C 64.30, H 7.68, N 23.07; found: C 64.08, H 7.81, N 22.77.

1,5-Di-3-((1-(2-pyridylethyl)amino)methylene)-1*H*-pyrazol-1-yl)-pentane (1b): Compound **1b** was synthesized according to the procedure described for compound **1a**. Instead of compound **8a**, compound **8b** (194 mg, 746 μmol) was used. The desired product was obtained as dark yellow, very viscous oil (166 mg, 351 μmol, 47%). ^{1}H NMR (500.1 MHz, $CDCl_3$): δ = 8.49 (ddd, ^5J = 0.9 Hz, ^4J = 1.9 Hz, ^3J = 5.0 Hz, 2H, C_{py}-*H*6), 7.56 (td, ^4J = 1.9 Hz, ^3J = 7.7 Hz, 2H, C_{py}-*H*4), 7.22 (d, ^3J = 2.2 Hz, 2H, C_{pz}-*H*5), 7.17-7.14 (m, 2H, C_{py}-*H*3), 7.09 (ddd, ^4J = 1.2 Hz, ^3J = 7.6 Hz, ^3J = 4.9 Hz, 2H, C_{py}-*H*5), 6.13 (d, ^3J = 2.2 Hz, 2H, C_{pz}-*H*4), 4.00 (t, ^3J = 7.1 Hz, 4H, $(N_{pz}CH_2CH_2)_2CH_2$), 3.83 (s, 4H, C_{pz}-CH_2NH_2), 3.09-3.05 (m, 4H, C_{py}-CH_2CH_2), 3.03-2.97 (m, 4H, C_{py}-CH_2CH_2), 2.53 (br s, 2H, N*H*), 1.81 (p, ^3J = 7.3 Hz, 4H, $(N_{pz}CH_2CH_2)_2CH_2$), 1.28-1.18 (m, 2H, $(N_{pz}CH_2CH_2)_2CH_2$) ppm; ^{13}C NMR (125.8 MHz, $CDCl_3$): δ = 160.3 (C_{py}-2), 151.0 (C_{pz}-3), 149.4 (C_{py}-6), 136.5 (C_{py}-4), 129.9 (C_{pz}-5), 123.4 (C_{py}-3), 121.4 (C_{py}-5), 104.3 (C_{pz}-4), 51.8 ($(N_{pz}CH_2CH_2)_2CH_2$), 49.0 (C_{py}-CH_2CH_2), 47.1 (C_{pz}-CH_2NH), 38.2 (C_{py}-CH_2CH_2), 30.0 ($(N_{pz}CH_2CH_2)_2CH_2$), 23.8 ($(N_{pz}CH_2CH_2)_2CH_2$) ppm; IR (neat): 3365 (br, s), 3270 (br, s), 3015 (vw), 2934 (w), 2850 (w), 1645 (w), 1590 (s), 1566 (w), 1518 (w), 1482 (s), 1434 (vs), 1363 (w), 1311 (w), 1203 (w), 1147 (w), 1103 (s), 1052 (s), 1003 (s), 761 (br, vs), 629 (br, s) cm^{-1}; HRMS (ESI): *m/z* calcd for $C_{27}H_{36}N_8 + H^+$: 473.31357 $[M+H]^+$; found: 473.31316; elemental analysis calcd (%) for $C_{27}H_{36}N_8 \cdot 1.8H_2O$: C 64.21, H 7.90, N 22.19; found: C 64.37, H 7.50, N 21.75.

1,4-Di-3-((1-(2-pyridylethyl)imino)methylene)-1*H*-pyrazol-1-yl)-butane (2a): Under inert atmosphere, 2-(2-pyridyl)ethylamine (140 μL, 1.17 mmol) was added to a mixture of compound **8a** (146 mg, 592 μmol) in toluene (8 mL) and molecular sieve 3 Å. The reaction mixture was stirred for 18 h at room temperature. Afterwards, the reaction mixture was filtered using a syringe filter. The solvent was evaporated under reduced pressure and the residue dried in vacuo to obtain the desired product as dark yellow oil, which slowly crystallizes (245 mg, 539 μmol, 91%). ^{1}H NMR (400.1 MHz, CD_2Cl_2): δ = 8.51 (ddd, ^5J = 1.0 Hz, ^4J = 1.9 Hz, ^3J = 4.9 Hz, 2H, C_{py}-*H*6), 8.23 (tt, ^5J = 0.6 Hz, ^4J = 1.3 Hz, 2H, C_{pz}-*CH*N), 7.57 (td„ ^4J = 1.9 Hz, ^3J = 7.6 Hz, 2H, C_{py}-*H*4), 7.33 (dd, ^5J = 0.7 Hz, ^3J = 2.4 Hz, 2H, C_{pz}-*H*5), 7.20–7.16 (m, 2H, C_{py}-*H*5), 7.12–7.08 (m, 2H, C_{py}-*H*3), 6.61 (dd, ^4J = 0.4 Hz, ^3J = 2.4 Hz, 2H, C_{pz}-*H*4), 4.12–4.07 (m, 4H, $N_{pz}CH_2(CH_2)_2CH_2N_{pz}$), 3.94 (ddd, ^4J = 1.4 Hz, ^3J = 7.1 Hz, 4H, C_{py}-CH_2CH_2), 3.12 (t, ^3J = 7.3 Hz, 4H, C_{py}-CH_2CH_2), 1.86–1.80 (m, 4H, $N_{pz}CH_2(CH_2)_2CH_2N_{pz}$) ppm; ^{13}C NMR (100.6 MHz, CD_2Cl_2(+$CDCl_3$)): δ = 160.1 (C_{py}-2), 155.5 (C_{pz}CHN), 150.5 (C_{pz}-3), 149.3 (C_{py}-6), 136.1 (C_{py}-4), 130.6 (C_{pz}-5), 123.5 (C_{py}-3), 121.2 (C_{py}-5), 104.0 (C_{pz}-4), 61.2 (C_{py}-CH_2CH_2), 51.9 ($N_{pz}CH_2(CH_2)_2CH_2N_{pz}$), 39.7 ($C_{py}$-$CH_2CH_2$), 27.5 ($N_{pz}CH_2(CH_2)_2CH_2N_{pz}$) ppm; IR (neat): 3120 (w), 3063 (w), 3012 (w), 2939 (m), 2924 (m), 2903 (m), 2876 (m), 2840 (m), 1726 (vw), 1706 (vw), 1639 (s), 1591 (s), 1573 (m), 1507 (m), 1471 (s), 1437 (vs), 1391 (m), 1381 (m), 1349 (s), 1329 (m), 1295 (m), 1278 (m), 1259 (m), 1211 (vs), 1181 (m), 1148 (m), 1103 (m), 1069 (m), 1051 (vs), 1023 (s), 997 (s), 979 (s), 963 (m), 952 (m), 870 (m), 800 (m), 771 (vs), 762 (vs), 747 (vs), 737 (vs), 692 (m), 629 (m), 589 (m), 529 (m), 496 (m), 454 (w) cm^{-1}; HRMS (ESI): *m/z* calcd for $C_{26}H_{30}N_8 + H^+$: 455.26662 $[M+H]^+$; found: 455.26615, *m/z* calcd for $C_{26}H_{30}N_8 + Na^+$: 477.24856 $[M+Na]^+$; found: 477.24807.

1,5-Di-3-((1-(2-pyridylethyl)imino)methylene)-1*H*-pyrazol-1-yl)-pentane (2b): Compound **2b** was synthesized according to the procedure described for compound **2a**. Instead of compound **8a**, compound **8b** (85.3 mg, 328 μmol) was used. The desired product was obtained as yellow, very viscous oil (143 mg, 305 μmol, 93%). ^{1}H NMR (400.1 MHz, CD_2Cl_2): δ = 8.51 (ddd, ^5J = 1.0 Hz, ^4J = 1.9 Hz, ^3J = 4.9 Hz, 2H, C_{py}-*H*6), 8.25-8.22 (m, 2H, C_{pz}-*CH*N), 7.58 (td„ ^4J = 1.9 Hz, ^3J = 7.7 Hz, 2H, C_{py}-*H*4), 7.33 (dd, ^5J = 0.7 Hz, ^3J = 2.4 Hz, 2H, C_{pz}-*H*5), 7.19 (ddd, ^5J = 0.8 Hz, ^4J = 1.4 Hz, ^3J = 7.8 Hz, 2H, C_{py}-*H*5), 7.13–7.08 (m, 2H, C_{py}-*H*3), 6.60 (dd, ^4J = 0.4 Hz, ^3J = 2.3 Hz, 2H, C_{pz}-*H*4), 4.08 (t, ^3J = 7.1 Hz, 4H, $(N_{pz}CH_2CH_2)_2CH_2$), 3.94 (td, ^4J = 1.4 Hz, ^3J = 7.3 Hz, 4H, C_{py}-CH_2CH_2), 3.12 (t, ^3J = 7.3 Hz, 4H, C_{py}-CH_2CH_2), 1.91–1.80 (m, 4H, $(N_{pz}CH_2CH_2)_2CH_2$), 1.34–1.20 (m, 2H, $(N_{pz}CH_2CH_2)_2CH_2$) ppm; ^{13}C NMR (100.6 MHz, CD_2Cl_2(+$CDCl_3$)): δ = 160.6 (C_{py}-2), 156.3 (C_{pz}CHN), 150.8 (C_{pz}-3), 149.9 (C_{py}-6), 136.8 (C_{py}-4), 131.1 (C_{pz}-5), 124.1 (C_{py}-3), 121.9 (C_{py}-5), 104.8 (C_{pz}-4), 61.9 (C_{py}-CH_2CH_2), 52.9 ($(N_{pz}CH_2CH_2)_2CH_2$), 40.3 (C_{py}-CH_2CH_2), 30.4 ($(N_{pz}CH_2CH_2)_2CH_2$), 24.3 ($(N_{pz}CH_2CH_2)_2CH_2$) ppm; IR (neat): 3063 (vw), 3002 (w), 2931 (m), 2855 (m), 1736 (w), 1652 (s), 1592 (s), 1567 (m), 1507 (m), 1471 (s), 1437 (s), 1383 (sh, m), 1355 (m), 1302 (m), 1215 (s), 1151 (m), 1103 (m), 1048 (s), 997 (m), 958 (w), 934 (vw), 895 (vw), 878 (vw), 843 (vw), 765 (vs), 695 (vw), 629 (m), 611 (w), 589 (w), 517 (w) cm^{-1}; HRMS (ESI): *m/z* calcd for $C_{27}H_{32}N_8 + H^+$: 469.28227 $[M+H]^+$; found: 469.28204.

MO4-PF$_6$ (3a): Since the isolation of compound **3a** as solid is not possible, the complex was freshly synthesized *in situ* by adding a solution of $[Cu(CH_3CN)_2]PF_6$ (2 eq.) in dichloromethane to a solution of compound **1a** (1 eq.) in dichloromethane. ^{1}H NMR (400.1 MHz, CD_2Cl_2 and small amounts of CD_3CN): δ = 8.45–8.31 (m, 2H, C_{py}-*H*6), 7.76–7.64 (m, 4H, C_{pz}-*H*5, C_{py}-*H*4), 7.48 (d, ^3J = 2.3 Hz, 2H, C_{py}-*H*3), 7.29–7.18 (m, 2H, C_{py}-*H*5), 6.36 (s, 2H, C_{pz}-*H*4), 4.27 (br. s 4H, C_{py}-CH_2CH_2),), 4.15 (t, ^3J = 6.8 Hz, 4H, $N_{pz}CH_2(CH_2)_2CH_2N_{pz}$), 3.42 (br. s, 4H, C_{pz}-CH_2NH), 3.17 (br. s, 4H, C_{py}-CH_2CH_2), 2.84 (s, 2H, N*H*), 1.92 (s, 6H, NCC*H*$_3$), 1.80–1.70 (m, 4H, $N_{pz}CH_2(CH_2)_2CH_2N_{pz}$) ppm.

MO5-PF$_6$ (4a): Since the isolation of compound **4a** as solid is not possible, the complex was freshly synthesized *in situ* by adding a solution of $[Cu(CH_3CN)_2]PF_6$ (2 eq.) in acetonitrile (2 mL) to a solution of compound **1b** (1 eq.). ^{1}H NMR (400.1 MHz, CD_2Cl_2 and small amounts of CD_3CN): δ = 8.49–8.31 (m, 2H, C_{py}-*H*6), 7.73–7.66 (m, 2H, C_{py}-*H*4), 7.47–7.38 (m, 2H, C_{pz}-*H*5), 7.31–7.15 (m, 4H, C_{py}-*H*3, C_{py}-*H*5), 6.23 (s, 2H, C_{pz}-*H*4), 4.07 (br. s, 8H, $N_{pz}(CH_2CH_2)_2CH_2$, C_{py}-CH_2CH_2), 3.18 (br. s, 4H, C_{pz}-CH_2NH), 2.97 (br. s, 4H, C_{py}-CH_2CH_2), 2.77 (s, 2H, N*H*), 1.92 (s, 6H, NCC*H*$_3$), 1.84–1.66 (m, 6H, $N_{pz}(CH_2CH_2)_2CH_2$), 1.23–1.19 (m, 2H, $N_{pz}(CH_2CH_2)_2CH_2$) ppm.

MO4im-PF$_6$ (5a): A solution of $[Cu(CH_3CN)_2]PF_6$ (78.16 mg, 209.7 μmol) in acetonitrile (2 mL) was added to a solution of **L^{MO4im}** (**2a**) (47.66 mg, 104.9 μmol) in acetonitrile (2 mL). The dark orange solution was stirred for 20 minutes. Removal of the solvent led to compound **5a** as a dark orange powder (83.87 mg, 89.00 μmol,

Research Article
doi.org/10.1002/ejic.202200509

85 %). ^{1}H NMR (400.1 MHz, CD_3CN): δ = 8.36–8.24 (m, 4H, C_{py}-*H*6, C_{pz}*CH*N C_{py}-*H*4), 7.71 (t, ^3J = 7.6 Hz, 2H,C_{py}-*H*3), 7.49 (d, ^3J = 2.4 Hz, 2H, C_{pz}-*H*5), 7.30–7.16 (m, 4H, C_{py}-*H*5), 6.81 (s, 2H, C_{pz}-*H*4), 4.07–3.94 (m. 8H, C_{py}-CH_2CH_2), 4.10 (br. s, 4H, $N_{pz}CH_2(CH_2)_2CH_2N_{pz}$), 3.16 (t, ^3J = 5.7 Hz, 4H, C_{py}-CH_2CH_2), 1.96 (s, 6H, $NCCH_3$), 1.63 (s, 4H, $N_{pz}CH_2(CH_2)_2CH_2N_{pz}$) ppm; ^{13}C NMR (100.6 MHz, CD_3CN): δ = 160.7 (C_{pz}*C*HN), 157.8 (C_{py}-2), 150.1 (C_{py}-6), 148.6 (C_{pz}-3), 138.6 (C_{py}-4), 132.9 (C_{pz}-5), 125.4 (C_{py}-3), 123.4 (C_{py}-5), 118.3 ($NCCH_3$), 107.0 (C_{pz}-4), 60.3 (C_{py}-CH_2CH_2), 52.7 ($N_{pz}CH_2(CH_2)_2CH_2N_{pz}$), 38.8 ($C_{py}$-$CH_2CH_2$), 27.5 ($N_{pz}CH_2(CH_2)_2CH_2N_{pz}$), 1.62 ($NCCH_3$) ppm; IR (neat): 3145 (vw), 2939 (vw), 2858 (vw), 1631 (sh, w), 1606 (m), 1570 (w), 1479 (m), 1440 (m), 1362 (m), 1310 (w), 1259 (vw), 1211 (w), 1163 (vw), 1105 (vw), 1069 (w), 1027 (w), 876 (w), 831 (vs), 765 (s), 589 (vw), 562 (vs) cm^{-1}; HRMS (ESI): *m/z* calcd for $C_{26}H_{30}N_8Cu_2^{2+}$: 290.05872 $[M]^{2+}$; found: 290.05843.

MO4im-[Alpftb)$_4$] (5 b): A solution of [Cu(*o*DFB)$_2$][Al(pftb)$_4$] (80.15 mg, 63.67 μmol) in dichloromethane (2 mL) was added to a solution of $\mathbf{L}^{\mathbf{MO4im}}$ (**2 a**) (14.47 mg, 31.83 μmol) in dichloromethane (2 mL). The bright yellow solution was stirred for 20 minutes. Removal of the solvent led to compound **5 b** as a dark yellow powder (53.43 mg, 21.24 μmol, 67 %). ^{1}H NMR (400.1 MHz, CD_2Cl_2): δ = 8.11-8.04 (m, 4H, C_{py}-*H*6, C_{py}-*H*4), 7.90 (d, ^5J = 0.6 Hz, ^4J = 1.3 Hz, 2H, C_{pz}*CH*N), 7.70 (d, ^3J = 2.5 Hz, 2H, C_{pz}-*H*5), 7.68–7.64 (m, 2H, C_{py}-*H*3), 7.44–7.36 (m, 2H, C_{py}-*H*5), 6.67 (d, ^3J = 2.4 Hz, 2H, C_{pz}-*H*4), 4.80–4.20 (br. s 4H, C_{py}-CH_2CH_2), 4.10 (br. s, 4H, $N_{pz}CH_2(CH_2)_2CH_2N_{pz}$), 3.88 (br. s, 4H, C_{py}-CH_2CH_2), 1.71 (br. s, 4H, $N_{pz}CH_2(CH_2)_2CH_2N_{pz}$) ppm; ^{13}C NMR (100.6 MHz, CD_2Cl_2): δ = 160.6 (C_{pz}CHN), 158.6 (C_{py}-2), 149.6 (C_{py}-6), 147.2 (C_{pz}-3), 142.1 (C_{py}-4), 136.2 (C_{pz}-5), 127.1 (C_{py}-3), 125.2 (C_{py}-5), 123.3 (q, $[Al(OC(CF_3)_3)_4]$), 111.4 (C_{pz}-4), 79.4 ($[Al(OC(CF_3)_3)_4]$), 61.9 (C_{py}-CH_2CH_2), 52.8 ($N_{pz}CH_2(CH_2)_2CH_2N_{pz}$), 42.7 ($C_{py}$-$CH_2CH_2$), 24.5 ($N_{pz}CH_2(CH_2)_2CH_2N_{pz}$) ppm; ^{19}F-NMR (376.5 MHz, CD_2Cl_2): δ =-76.2 ($[Al(OC(CF_3)_3)_4]$) ppm; ^{27}Al (104.3 MHz, CD_2Cl_2): δ = 33.3 ($[Al(OC(CF_3)_3)_4]$) ppm; IR (neat): 2964 (w), 2921 (vw), 1642 (w), 1613 (w), 1489 (vw), 1446 (vw), 1352 (m), 1298 (s), 1271 (s), 1242 (vs), 1211 (vs), 1165 (s), 1105 (m), 1076 (m), 1036 (m), 1021 (m), 967 (vs), 867 (vw), 831 (sh, m), 804 (m), 771 (m), 755 (w), 726 (vs), 605 (vw), 563 (m), 538 (s), 447 (s) cm^{-1}; FT-Raman (solid): 2965 (w), 2905 (w), 1643 (s), 1609 (w), 1514 (w), 1356 (m), 1234 (w), 1037 (m), 800 (m), 749 (m), 534 (w) cm^{-1}.

MO5im-PF_6 (6 a): $[Cu(CH_3CN)_2]PF_6$ (78.95 mg, 211.8 μmol) was dissolved in acetonitrile (3 mL). 2.1 mL of this solution was added to a solution of $\mathbf{L}^{\mathbf{MO4im}}$ (**2 a**) (35.34 mg, 75.42 μmol) in acetonitrile (2 mL). The dark orange solution was stirred for 20 minutes. Removal of the solvent led to compound **6 a** as a dark yellow powder (63.59 mg, 65.71 μmol, 87 %). ^{1}H NMR (400.1 MHz, CD_3CN): δ = 8.39 (s, 2H, C_{pz}-*CH*N), 8.13 (s, 2H, C_{py}-*H*6), 7.63 (dd, ^3J = 6.5 Hz, ^3J = 8.2 Hz, 2H, C_{py}-*H*4), 7.39 (d, ^3J = 2.3 Hz, 2H, C_{pz}-*H*5), 7.19 (d, ^3J = 7.8 Hz, 2H, C_{py}-*H*3), 7.12 (t, ^3J = 6.4 Hz, 2H, C_{py}-*H*5), 6.62 (d, ^3J = 2.4 Hz, 2H, C_{pz}-*H*4), 4.14 (s 4H, C_{py}-CH_2CH_2), 3.89-3.77 (m, 4H, $N_{pz}(CH_2CH_2)_2CH_2$), 3.19 (br. s, 4H, C_{py}-CH_2CH_2), 1.96 (s, 6H, $NCCH_3$), 1.71 (br. s, 4H, $N_{pz}(CH_2CH_2)_2CH_2$), 0.79-0.68 (m, 2H, $N_{pz}(CH_2CH_2)_2CH_2$) ppm; ^{13}C NMR (100.6 MHz, CD_3CN): δ = 160.6 (C_{pz}*C*HN), 158.0 (C_{py}-2), 149.8 (C_{py}-6), 148.5 (C_{pz}-3), 138.1 (C_{py}-4), 132.9 (C_{pz}-5), 125.0 (C_{py}-3), 123.1 (C_{py}-5), 118.3 ($NCCH_3$), 106.7 (C_{pz}-4), 60.7 (C_{py}-CH_2CH_2), 53.0 ($(N_{pz}CH_2CH_2)_2CH_2$), 39.0 (C_{py}-CH_2CH_2), 29.7 ($(N_{pz}CH_2CH_2)_2CH_2$), 23.6 ($(N_{pz}CH_2CH_2)_2CH_2$),1.62 ($NCCH_3$) ppm; IR (neat): 3145 (vw), 2933 (w), 2861 (w), 1740 (vw), 1630 (w), 1596 (m), 1570 (w), 1507 (vw), 1476 (m), 1443 (m), 1362 (m), 1313 (m), 1259 (w), 1214 (m), 1159 (w), 1103 (w), 1061 (m), 1030 (w), 997 (vw), 948 (vw), 874 (m), 831 (vs), 758 (s), 634 (w), 587 (w), 559 (vs) cm^{-1}; HRMS (ESI): *m/z* calcd for $C_{27}H_{32}N_8Cu_2^{2+}$: 297.06655 $[M]^{2+}$; found: 297.06629.

MO5im-[Alpftb)$_4$] (6 b): [Cu(*o*DFB)$_2$][Al(pftb)$_4$] (79.61 mg, 63.67 μmol) was dissolved in dichloromethane (2 mL). 0.92 mL of this solution was added to a solution of $\mathbf{L}^{\mathbf{MO4im}}$ (**2 a**) (6.84 mg, 14.60 μmol) in dichloromethane (2 mL). The bright yellow solution was stirred for 20 minutes. Removal of the solvent led to compound **6 b** as a dark yellow powder (28.70 mg, 11.34 μmol, 77 %). ^{1}H NMR (400.1 MHz, CD_2Cl_2): δ = 8.28-8.24 (m, 2H, C_{py}-*H*6), 8.10 (td, ^4J = 1.7 Hz, ^3J = 7.8 Hz, 2H, C_{py}-*H*4), 8.01 (s, 2H, C_{pz}-*CH*N), 7.69 (d, ^3J = 2.5 Hz, 2H, C_{pz}-*H*5), 7.68–7.65 (m, 2H, C_{py}-*H*3), 7.46 (ddd, ^3J = 1.4 Hz, ^3J = 5.6 Hz, ^4J = 7.7 Hz, 2H, C_{py}-*H*5), 6.70 (d, ^3J = 2.5 Hz, 2H, C_{pz}-*H*4), 4.62–3.96 (br. m, 8H, C_{py}-CH_2CH_2, $N_{pz}(CH_2CH_2)_2CH_2$), 3.84 (br. s, 4H, C_{py}-CH_2CH_2), 1.57 (br. s, 4H, $N_{pz}(CH_2CH_2)_2CH_2$), 1.10-0.96 (m, 2H, $N_{pz}(CH_2CH_2)_2CH_2$) ppm; ^{13}C NMR (100.6 MHz, CD_2Cl_2): δ = 160.8 (C_{pz}*C*HN), 159.0 (C_{py}-2), 150.0 (C_{py}-6), 146.7 (C_{pz}-3), 142.1 (C_{py}-4), 135.2 (C_{pz}-5), 126.9 (C_{py}-3), 125.3 (C_{py}-5), 121.9 (q, $[Al(OC(CF_3)_3)_4]$), 111.6 (C_{pz}-4), 79.5 ($[Al(OC(CF_3)_3)_4]$), 62.1 (C_{py}-CH_2CH_2), 55.1 ($(N_{pz}CH_2CH_2)_2CH_2$), 42.6 (C_{py}-CH_2CH_2), 29.0 ($(N_{pz}CH_2CH_2)_2CH_2$), 25.8 ($(N_{pz}CH_2CH_2)_2CH_2$) ppm; ^{19}F-NMR (376.5 MHz, CD_2Cl_2): δ =-76.2 ($[Al(OC(CF_3)_3)_4]$) ppm; ^{27}Al (104.3 MHz, CD_2Cl_2): δ = 33.6 ($[Al(OC(CF_3)_3)_4]$) ppm; IR (neat): 2960 (w), 2924 (vw), 1642 (w), 1613 (w), 1489 (vw), 1446 (vw), 1352 (m), 1298 (s), 1271 (s), 1242 (vs), 1211 (vs), 1165 (s), 1096 (m), 1024 (m), 967 (vs), 867 (vw), 800 (s), 776 (m), 758 (w), 726 (vs), 562 (m), 538 (s), 447 (s) cm^{-1}; FT-Raman (solid): 2962 (w), 2905 (w), 1640 (s), 1616 (w), 1374 (w), 1034 (m), 797 (m), 746 (m), 564 (w), 540 (w) cm^{-1}.

Deposition Number 2156795 (for **5 a**) contains the supplementary crystallographic data for this paper. These data are provided free of charge by the joint Cambridge Crystallographic Data Centre and Fachinformationszentrum Karlsruhe Access Structures service www.ccdc.cam.ac.uk/structures.

Acknowledgements

The authors thank I. Krossing and M. Schmitt, University of Freiburg, for the provision with [NO][Al(OC(CF$_3$)$_3$)$_4$] and the spectroscopic department of the Institute of Inorganic Chemistry for measurements, as well as CAU Kiel for financial support of this research. Open Access funding enabled and organized by Projekt DEAL.

Conflict of Interest

The authors declare no conflict of interest.

Data Availability Statement

The data that support the findings of this study are available in the supplementary material of this article.

Keywords: Catalysis · Copper · Dinuclear Complex · Ligand Rigidity · Tyrosinase

[1] a) L. Cerenius, K. Söderhäll, *Dev. Comp. Immunol.* **2021**, *122*, 104098; b) J.-S. Taylor, *Science* **2015**, *347*, 824; c) C. J. Coates, J. Nairn, *Dev. Comp. Immunol.* **2014**, *45*, 43.
[2] L. Marais, H. C. M. Vosloo, A. J. Swarts, *Coord. Chem. Rev.* **2021**, *440*, 213958.
[3] H. Decker, T. Schweikardt, F. Tuczek, *Angew. Chem. Int. Ed.* **2006**, *45*, 4546.
[4] C. E. Elwell, N. L. Gagnon, B. D. Neisen, D. Dhar, A. D. Spaeth, G. M. Yee, W. B. Tolman, *Chem. Rev.* **2017**, *117*, 2059.

[5] M. Rolff, J. Schottenheim, H. Decker, F. Tuczek, *Chem. Soc. Rev.* **2011**, *40*, 4077.
[6] J. N. Hamann, B. Herzigkeit, R. Jurgeleit, F. Tuczek, *Coord. Chem. Rev.* **2017**, *334*, 54.
[7] E. I. Solomon, D. E. Heppner, E. M. Johnston, J. W. Ginsbach, J. Cirera, M. Qayyum, M. T. Kieber-Emmons, C. H. Kjaergaard, R. G. Hadt, L. Tian, *Chem. Rev.* **2014**, *114*, 3659.
[8] R. Trammell, K. Rajabimoghadam, I. Garcia-Bosch, *Chem. Rev.* **2019**, *119*, 2954.
[9] a) Y. Matoba, S. Kihara, Y. Muraki, N. Bando, H. Yoshitsu, T. Kuroda, M. Sakaguchi, K.'e. Kayama, H. Tai, S. Hirota et al., *Biochemistry* **2017**, *56*, 5593; b) Y. Matoba, T. Kumagai, A. Yamamoto, H. Yoshitsu, M. Sugiyama, *J. Biol. Chem.* **2006**, *281*, 8981.
[10] a) E. Lo Presti, M. L. Perrone, L. Santagostini, L. Casella, E. Monzani, *Inorg. Chem.* **2019**, *58*, 7335; b) M. L. Perrone, E. Salvadeo, E. Lo Presti, L. Pasotti, E. Monzani, L. Santagostini, L. Casella, *Dalton Trans.* **2017**, *46*, 4018.
[11] a) W. Keown, J. B. Gary, T. D. P. Stack, *J. Biol. Inorg. Chem.* **2017**, *22*, 289; b) L. M. Mirica, M. Vance, D. J. Rudd, B. Hedman, K. O. Hodgson, E. I. Solomon, T. D. P. Stack, *Science* **2005**, *308*, 1890.
[12] a) M. S. Askari, K. V. N. Esguerra, J.-P. Lumb, X. Ottenwaelder, *Inorg. Chem.* **2015**, *54*, 8665; b) M. S. Askari, L. A. Rodríguez-Solano, A. Proppe, B. McAllister, J.-P. Lumb, X. Ottenwaelder, *Dalton Trans.* **2015**, *44*, 12094.
[13] a) M. Paul, M. Teubner, B. Grimm-Lebsanft, C. Golchert, Y. Meiners, L. Senft, K. Keisers, P. Liebhäuser, T. Rösener, F. Biebl et al., *Chem. Eur. J.* **2020**, *26*, 7556; b) P. Liebhäuser, K. Keisers, A. Hoffmann, T. Schnappinger, I. Sommer, A. Thoma, C. Wilfer, R. Schoch, K. Stührenberg, M. Bauer et al., *Chem. Eur. J.* **2017**, *23*, 12171; c) S. Herres-Pawlis, U. Flörke, G. Henkel, *Eur. J. Inorg. Chem.* **2005**, 3815.
[14] R. Schneider, T. A. Engesser, C. Näther, I. Krossing, F. Tuczek, *Angew. Chem. Int. Ed.* **2022**, *61*, e202202562.
[15] K. D. Karlin, J. C. Hayes, Y. Gultneh, R. W. Cruse, J. W. McKown, J. P. Hutchinson, J. Zubieta, *J. Am. Chem. Soc.* **1984**, *106*, 2121.
[16] I. Garcia-Bosch, A. Company, J. R. Frisch, M. Torrent-Sucarrat, M. Cardellach, I. Gamba, M. Güell, L. Casella, L. Que, X. Ribas et al., *Angew. Chem. Int. Ed.* **2010**, *49*, 2406.
[17] J. Serrano-Plana, I. Garcia-Bosch, A. Company, M. Costas, *Acc. Chem. Res.* **2015**, *48*, 2397.
[18] K. Tabuchi, M. Z. Ertem, H. Sugimoto, A. Kunishita, T. Tano, N. Fujieda, C. J. Cramer, S. Itoh, *Inorg. Chem.* **2011**, *50*, 1633.
[19] J. E. Bulkowski, US-Patent 4.545.937, **1985**.
[20] M. Réglier, C. Jorand, B. Waegell, *J. Chem. Soc. Chem. Commun.* **1990**, *107*, 1752.
[21] J. Schottenheim, C. Gernert, B. Herzigkeit, J. Krahmer, F. Tuczek, *Eur. J. Inorg. Chem.* **2015**, 3501.
[22] L. Casella, M. Gullotti, M. Bartosek, G. Pallanza, E. Laurenti, *J. Chem. Soc. Chem. Commun.* **1991**, 1235.
[23] L. Casella, M. Gullotti, R. Radaelli, P. Di Gennaro, *J. Chem. Soc. Chem. Commun.* **1991**, 1611.
[24] L. Santagostini, M. Gullotti, E. Monzani, L. Casella, R. Dillinger, F. Tuczek, *Chem. Eur. J.* **2000**, *6*, 519.
[25] M. Rolff, J. Schottenheim, G. Peters, F. Tuczek, *Angew. Chem.* **2010**, *122*, 6583.
[26] a) J. N. Hamann, R. Schneider, F. Tuczek, *J. Coord. Chem.* **2015**, *68*, 3259; b) J. N. Hamann, F. Tuczek, *Chem. Commun.* **2014**, *50*, 2298; c) J. Schottenheim, N. Fateeva, W. Thimm, J. Krahmer, F. Tuczek, *Z. Anorg. Allg. Chem.* **2013**, *639*, 1491; d) M. Rolff, J. Schottenheim, G. Peters, F. Tuczek, *Angew. Chem. Int. Ed.* **2010**, *49*, 6438.
[27] a) A. De, S. Mandal, R. Mukherjee, *J. Inorg. Biochem.* **2008**, *102*, 1170; b) O. Sander, A. Henss, C. Näther, C. Würtele, M. C. Holthausen, S. Schindler, F. Tuczek, *Chem. Eur. J.* **2008**, *14*, 9714; c) S. P. Foxon, D. Utz, J. Astner, S. Schindler, F. Thaler, F. W. Heinemann, G. Liehr, J. Mukherjee, V. Balamurugan, D. Ghosh and R. Mukherjee, *Dalton Trans.* **2004**, 2321.
[28] S. Thyagarajan, N. N. Murthy, A. A. Narducci Sarjeant, K. D. Karlin, S. E. Rokita, *J. Am. Chem. Soc.* **2006**, *128*, 7003.
[29] E. Lee, Y. An, J. Kwon, K. I. Kim, R. Jeon, *Bioorg. Med. Chem.* **2017**, *25*, 3614.
[30] W. L. Driessen, J. E. Bol, B. Maase, G. Gonesh, K. Goubitz, J. Reedijk, *Heterocycles* **1997**, *45*, 1477.
[31] a) G. Santiso-Quiñones, A. Higelin, J. Schaefer, R. Brückner, C. Knapp, I. Krossing, *Chemistry* **2009**, *15*, 6663; b) I. Krossing, A. Reisinger, *Coord. Chem. Rev.* **2006**, *250*, 2721; c) I. Krossing, *J. Am. Chem. Soc.* **2001**, *123*, 4603.
[32] L. M. Mirica, X. Ottenwaelder, T. D. P. Stack, *Chem. Rev.* **2004**, *104*, 1013.
[33] E. I. Solomon, J. W. Ginsbach, D. E. Heppner, M. T. Kieber-Emmons, C. H. Kjaergaard, P. J. Smeets, L. Tian, J. S. Woertink, *Faraday Discuss.* **2011**, *148*, 11–39.
[34] K. V. N. Esguerra, Y. Fall, L. Petitjean, J.-P. Lumb, *J. Am. Chem. Soc.* **2014**, *136*, 7662.
[35] B. Herzigkeit, R. Jurgeleit, B. M. Flöser, N. E. Meißner, T. A. Engesser, C. Näther, F. Tuczek, *Eur. J. Inorg. Chem.* **2019**, 2258.
[36] C. Imbert, H. P. Hratchian, M. Lanznaster, M. J. Heeg, L. M. Hryhorczuk, B. R. McGarvey, H. B. Schlegel, C. N. Verani, *Inorg. Chem.* **2005**, *44*, 7414.
[37] T. Inoue, Y. Shiota, K. Yoshizawa, *J. Am. Chem. Soc.* **2008**, *130*, 16890.
[38] M. Gude, C. Hubschwerken, US 2014/0038961 A1.
[39] G. M. Sheldrick, *Acta Crystallogr.* **2015**, *A71*, 3.
[40] G. M. Sheldrick, *Acta Crystallogr.* **2015**, *C71*, 3.
[41] a) F. Neese, F. Wennmohs, U. Becker, C. Riplinger, *J. Chem. Phys.* **2020**, *152*, 224108-224108-18; b) F. Neese, *Wiley Interdiscip. Rev.: Comput. Mol. Sci.* **2018**, *8*, e1327; c) F. Neese, *Wiley Interdiscip. Rev.: Comput. Mol. Sci.* **2012**, *2*, 73.
[42] A. D. Becke, *J. Chem. Phys.* **1993**, *98*, 5648.
[43] F. Weigend, R. Ahlrichs, *Phys. Chem. Chem. Phys.* **2005**, *7*, 3297.
[44] F. Neese, F. Wennmohs, A. Hansen, U. Becker, *Chem. Phys.* **2009**, *356*, 98.
[45] F. Weigend, *Phys. Chem. Chem. Phys.* **2006**, *8*, 1057.
[46] a) S. Grimme, S. Ehrlich, L. Goerigk, *J. Comput. Chem.* **2011**, *32*, 1456; b) S. Grimme, J. Antony, S. Ehrlich, H. Krieg, *J. Chem. Phys.* **2010**, *132*, 154104.

Manuscript received: August 9, 2022
Revised manuscript received: September 16, 2022
Accepted manuscript online: September 19, 2022